

# Using satellite observations to evaluate model representation of Arctic mixed-phase clouds

Jonah K Shaw<sup>1,1</sup>, Zachary McGraw<sup>2,2</sup>, Olimpia Bruno<sup>3,3</sup>, Trude Storelvmo<sup>2,2</sup>, and Stefan Hofer<sup>2,2</sup>

<sup>1</sup>University of Colorado at Boulder

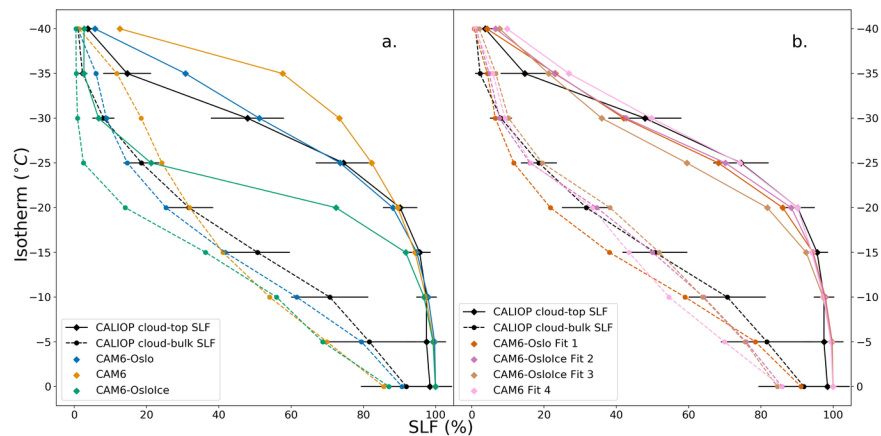
<sup>2</sup>University of Oslo

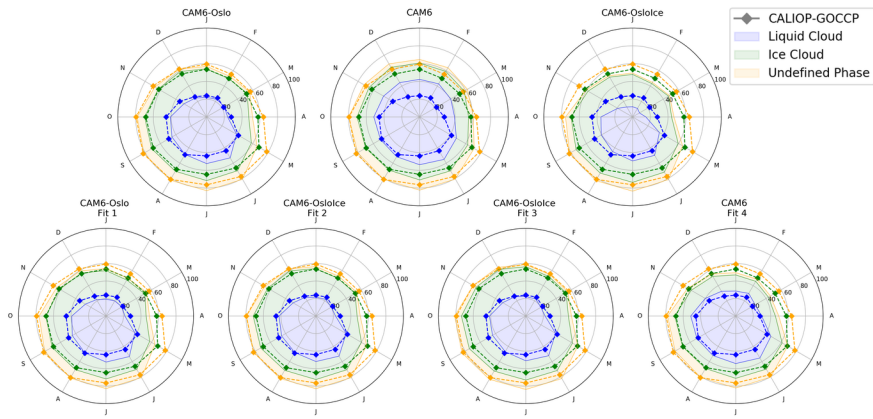
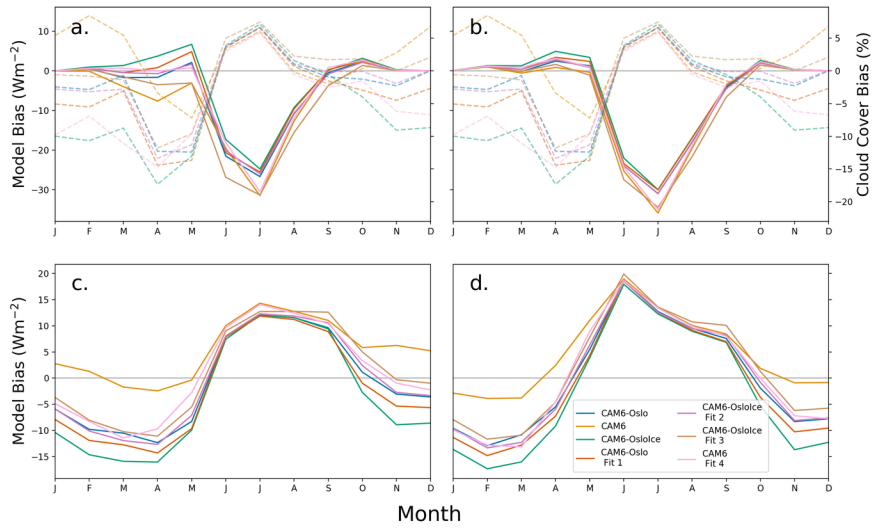
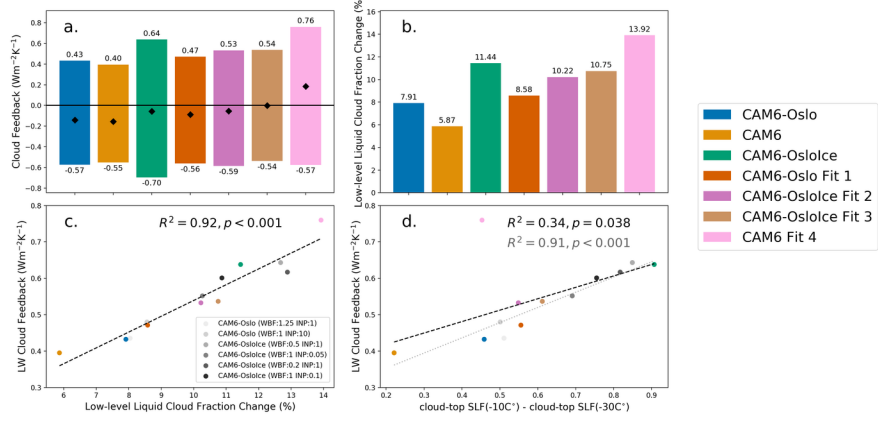
<sup>3</sup>Karlsruhe Institute of Technology

November 30, 2022

## Abstract

Clouds play an important role in determining Arctic warming, but remain difficult to constrain with available observations. We use two satellite-derived cloud phase metrics to investigate the vertical structure of Arctic clouds in global climate models that use the Community Atmosphere Model version 6 (CAM6) atmospheric component. We produce a set of constrained model runs by adjusting model microphysical variables to match the cloud phase metrics. Models in this small ensemble have variable representation of cloud amount and phase in the winter, while uniformly underestimating total cloud cover in the spring and overestimating it in the summer. We find a consistent correlation between winter and spring cloud cover simulated for the present-day and the longwave cloud feedback parameter.





1                   **Using satellite observations to evaluate model**  
2                   **microphysical representation of Arctic mixed-phase**  
3                   **clouds**

4                   **J. Shaw<sup>1\*</sup>, Z. S. McGraw<sup>1†</sup>, O. Bruno<sup>2</sup>, T. Storelvmo<sup>1,3</sup>, and S. Hofer<sup>1</sup>**

5                                   <sup>1</sup>Department of Geosciences, University of Oslo, Oslo, Norway

6                                   <sup>2</sup>Karlsruhe Institute of Technology, Institute of Meteorology and Climate Research

7                                   <sup>3</sup>School of Business, Nord University, Bodø, Norway

8                   **Key Points:**

- 9                   • CAM6-Oslo and CAM6 capture the vertical structure of Arctic mixed-phase clouds,  
10                   with supercooled liquid cloud tops overlying icy interiors.  
11                   • Removing an erroneous limit on heterogeneous and secondary ice nucleation pro-  
12                   cesses in CAM6 reduces supercooled liquid water in Arctic clouds.  
13                   • Parametrizations of mixed-phase processes control the longwave cloud feedback  
14                   parameter by modifying how winter and spring clouds respond to warming.

---

\*Now at Department of Atmospheric and Oceanic Sciences, University of Colorado at Boulder

†Now at Department of Applied Physics and Applied Mathematics, Columbia University and NASA  
Goddard Institute for Space Studies

Corresponding author: Jonah Shaw, [jonah.shaw@colorado.edu](mailto:jonah.shaw@colorado.edu)

**Abstract**

Mixed-phase clouds play an important role in determining Arctic warming, but are highly parametrized in models and difficult to constrain with observations. We use two satellite-derived cloud phase metrics to investigate the vertical structure of Arctic clouds in two global climate models that use the Community Atmosphere Model version 6 (CAM6) atmospheric component. We report a model error limiting ice nucleation, produce a set of Arctic-constrained model runs by adjusting model microphysical variables to match the cloud phase metrics, and evaluate cloud feedbacks for all simulations. Models in this small ensemble uniformly overestimate total cloud fraction in the summer, but have variable representation of cloud fraction and phase in the winter and spring. By relating modelled cloud phase metrics and changes in low-level liquid cloud amount under warming to longwave cloud feedback, we show that mixed-phase processes mediate the Arctic climate by modifying how wintertime and springtime clouds respond to warming.

**Plain Language Summary**

[ Clouds are important regulators of warming in the Arctic. The thermodynamic phase of a cloud affects its lifetime and transparency to incoming and outgoing radiation. As a result, transitions from ice to liquid in a warming climate change the influence of clouds on surface temperature. At temperatures between  $-37$  °C and  $0$  °C, both ice and supercooled liquid water may exist simultaneously in a cloud layer. Global climate models struggle to capture cloud phase in this temperature range because it depends on both cloud temperature and aerosol properties. This study investigates how the fraction of supercooled liquid water changes vertically in Arctic clouds, comparing liquid-rich cloud tops with their icy interiors. We describe a significant model error that limits the formation of new ice crystals. We also find that global climate models reproduce observations, and that a range of model parameters produce results consistent with observations. Changes in cloud fraction resulting from these adjustments mostly occur in the winter and spring, and cause the models to trap longwave radiation differently. The results of this study highlight the need to capture seasonal changes in cloud phase and amount in order to successfully predict future changes to the Arctic climate. ]

**1 Introduction**

Uncertainties in cloud and aerosol radiative effects are a principal contributor to climate model uncertainty, and remain so despite decades of model development (Boucher et al., 2013). These uncertainties arise from the difficulty of representing aerosol-cloud interactions and other key physical processes at the typical resolutions of global climate models (GCMs). Evaluations of available models from the Coupled Model Intercomparison Project Phase 6 (CMIP6) (Eyring et al., 2016) indicate that changes in climate sensitivity relative to CMIP5 (Taylor et al., 2012) are mostly due to changes in cloud representation, specifically for extratropical low-level clouds (Zelinka et al., 2020). Using observations to reevaluate the representation of these clouds in the latest generation of GCMs is a vital part of testing the validity of these new predictions.

In the Arctic, clouds mediate climate change through interactions with land and sea ice, and impacts on surface radiative fluxes (H. Morrison et al., 2012). As the thermodynamic phase of Arctic clouds shifts from ice to liquid in response to warming, the radiative effect they exert on the surface changes (Mitchell et al., 1989). This cloud phase feedback depends on cloud optical thickness and lifetime changes. In the Arctic, observations indicate that liquid and ice clouds exert very different radiative forcings on the surface (Shupe & Intrieri, 2004; Cesana et al., 2012), highlighting the need for models to capture cloud phase in order to produce a realistic surface energy budget.

63 At temperatures between approximately  $-37\text{ }^{\circ}\text{C}$  and  $0\text{ }^{\circ}\text{C}$ , cloud ice forms via het-  
64 erogeneous nucleation processes that are dependent on temperature, in-cloud vapor pres-  
65 sure, and the presence of ice nucleating particles (INPs) (Korolev, 2007). Cloud ice and  
66 water can coexist as mixed-phase clouds in this regime. The fraction of supercooled liq-  
67 uid water in a mixed-phase cloud layer can be referred to as the supercooled liquid frac-  
68 tion (SLF) (Komurcu et al., 2014). Observations show that Arctic mixed-phase clouds  
69 are both common and long-lived (Matus & L’Ecuyer, 2017; H. Morrison et al., 2012),  
70 due in part to their vertical structure in which INP-limited liquid cloud tops are sepa-  
71 rated from glaciated interiors, preventing ice from quickly depleting cloud water and al-  
72 lowing clouds to persist for several days (Hobbs & Rangno, 1998). Through this effect  
73 on cloud lifetime and opacity, cloudtop phase mediates the resulting long- and shortwave  
74 cloud feedbacks.

75 Model representation of mixed-phase clouds relies on uncertain parameters. Sev-  
76 eral studies of mixed-phase clouds in Version 5 of the Community Atmosphere Model  
77 (CAM5) have found that the Wegener–Bergeron–Findeisen (WBF) process time scale  
78 has the largest role in determining liquid cloud fraction (Tan & Storelvmo, 2016; McIl-  
79 hattan et al., 2017; Huang et al., 2021), with Huang et al. (2021) finding that reducing  
80 the WBF time scale was primarily important in INP-limited environments. High-resolution  
81 modelling studies of Arctic mixed-phase clouds also indicate that cloud phase is highly  
82 sensitive to ice formation mechanisms and the availability of INPs (Jiang et al., 2000;  
83 Fridlind et al., 2007; Fu et al., 2019). Because INP concentrations and the strength of  
84 the WBF process specifically impact mixed-phase clouds and have large reasonable ranges,  
85 they make appropriate tuning parameters for GCM experiments (Mauritsen et al., 2012).

86 Observations of cloud fraction and phase obtained from the Cloud-Aerosol Lidar  
87 with Orthogonal Polarization (CALIOP) sensor aboard the CALIPSO platform provide  
88 a strong observational constraint for assessing cloud representation in GCMs (Winker  
89 et al., 2009). Cloud phase is especially important, as observations of cloud fraction alone  
90 may hide compensating phase biases with large radiative impacts (Cesana & Chepfer,  
91 2012). Using CALIOP cloud phase products, Cesana et al. (2012) found that radiatively  
92 clear (opaque) atmospheric states in the Arctic were characterized by the absence (pres-  
93 ence) of liquid cloud. This result supported the findings of Shupe and Intrieri (2004) and  
94 demonstrated that satellite retrievals of cloud phase can be effectively used to study the  
95 Arctic surface energy budget.

96 Comparing CAM6 to cloud phase observations is enabled by the use of definition-  
97 and scale-aware cloud phase variables produced by the Cloud Feedback Model Intercom-  
98 parison Project (CFMIP) Observational Simulator Package: Version 2 (COSP2) (Swales  
99 et al., 2018). With new heterogeneous ice nucleation (Hoose et al., 2008) and stratiform  
100 cloud microphysics (H. Morrison & Gettelman, 2008) schemes in CAM6 causing signif-  
101 icant changes to precipitation and cloud fraction over the Greenland Ice Sheet (Lenaerts  
102 et al., 2020), further investigation of cloud representation over the entire Arctic region  
103 is well motivated.

104 Recent studies of Arctic feedbacks highlight the importance of the temperature and  
105 albedo feedbacks (Pithan & Mauritsen, 2014), noting the lack of a cloud response to sum-  
106 mer sea ice loss (A. L. Morrison et al., 2018). While longwave cloud feedbacks are be-  
107 lieved to play a secondary role in Arctic warming, large uncertainties associated with mixed-  
108 phase processes have yet to be evaluated.

109 In the Arctic, both CMIP5 models and reanalysis data products struggle to repro-  
110 duce observed cloud phase and optical depth (Lenaerts et al., 2017). Because many Arc-  
111 tic feedbacks are non-linear, this inability to capture the mean state influences projected  
112 cloud feedbacks (Goosse et al., 2018). Targeted modeling experiments which capture the  
113 observed mean state are valuable tools for disentangling the roles of different Arctic feed-  
114 back mechanisms and evaluating model parameterizations (Kay et al., 2016). Tan and

115 Storelvmo (2019) found that minimizing global cloud phase biases in the CESM1 model  
 116 yielded a broad range of cloud microphysical variables and Arctic Amplification factors.  
 117 This study, however, did not examine whether the global model adjustments created a  
 118 reasonable representation of cloud phase in the Arctic itself or distinguish between re-  
 119 mote and local drivers of Arctic feedbacks (Feldl et al., 2020). We address this concern  
 120 by focusing our model adjustments and analysis on the Arctic and assessing model per-  
 121 formance with additional observational constraints. Atmosphere-only simulations iso-  
 122 late how the microphysical representation of mixed-phase clouds impacts Arctic warm-  
 123 ing. Whereas the fully-coupled simulations of Tan and Storelvmo (2019) investigated the  
 124 Arctic impact of a global SLF correction, this work specifically investigates how and why  
 125 local cloud microphysics affect the Arctic.

## 126 2 Methods

### 127 2.1 Cloud Phase Metrics

128 To investigate the vertical structure of mixed-phase clouds, we filter by overlying  
 129 cloud optical thickness (COT) to produce two SLF metrics. We obtain one metric (here-  
 130 after: cloud-top SLF) by selecting only the highest layer of observed mixed-phase clouds  
 131 after discarding the uppermost layers with  $COT < 0.3$  in order to avoid including optically-  
 132 thin cirrus clouds. Another metric (hereafter: cloud-bulk SLF) is obtained by selecting  
 133 all cloud layers retrieved by CALIOP with overlying COT less than 3.0. Validation of  
 134 the cloud bulk metric, as well as methodology for calculating the observational and mod-  
 135 elled SLF metrics are described in the Supplementary Material. SLF is calculated on isotherms  
 136 from  $-40^{\circ}\text{C}$  to  $0^{\circ}\text{C}$ , with a  $5^{\circ}\text{C}$  increment. Measurements of cloud phase were retrieved  
 137 from NASA’s CALIOP instrument (Winker et al., 2009) for a four year observational  
 138 period from 1 June 2009 through 31 May 2013.

### 139 2.2 Additional Satellite Products

140 To conduct further model evaluation of cloud fraction and radiative fluxes, we com-  
 141 pare against the GCM-Oriented CALIPSO Cloud Product (GOCCP) Version 3 (Chepfer  
 142 et al., 2010) and Clouds and the Earth’s Radiant Energy System Energy Balanced and  
 143 Filled (CERES-EBAF) Ed4.0 datasets (Kato et al., 01 Jun. 2018). The GOCCP data  
 144 product ( $82^{\circ}\text{S}$  -  $82^{\circ}\text{N}$ ) separates total cloud fraction by phase, and is produced specif-  
 145 ically for comparison with the COSP satellite simulator. From CERES-EBAF, we use  
 146 computed surface long- and shortwave cloud radiative effect (CRE) values and surface  
 147 all-sky downwelling fluxes.

### 148 2.3 Modeling Simulations

149 We present atmosphere-only runs of the Nordic Earth System Model Version 2 (NorESM2)  
 150 (Seland et al., 2020) and the Community Earth System Model Version 2 (CESM2) (Danabasoglu  
 151 et al., 2020). Both models have 32 vertical levels and are run at  $1.9^{\circ} \times 2.5^{\circ}$  horizontal  
 152 resolution. We use identical model components in both GCMs to isolate the impact of  
 153 differences between the atmospheric modules. While both models use CAM6, CESM2  
 154 uses the MAM4 aerosol scheme (Liu et al., 2016), and NorESM2 uses the OsloAero5.3  
 155 (Kirkevåg et al., 2018) aerosol scheme while also parametrizing mid- and high-level ice  
 156 clouds differently. Runs of NorESM2 and CESM2 are subsequently referred to as CAM6-  
 157 Oslo and CAM6. All modelled data represent averages over the same 4-year period from  
 158 which SLF values were calculated following a 3-month model windup to allow the atmo-  
 159 sphere to adjust to microphysics changes. To reduce variability in meteorology between  
 160 runs, we nudge horizontal winds and surface pressure to ERA-Interim reanalysis data  
 161 for the observational period (Dee et al., 2011). Because sea ice concentrations are pre-  
 162 scribed, these simulations do not explore cloud-sea ice feedbacks.

163

## 2.4 Model Modifications

164

165

166

167

168

169

170

171

172

173

INP availability is an important limiting factor in cloud glaciation at mixed-phase temperatures. In CAM6 and CAM6-Oslo, the in-cloud ice number concentration cannot exceed the calculated concentration of available ice nuclei. Neither heterogeneous nor secondary nucleation processes contribute to this INP limit, preventing them from nucleating ice crystals. Heterogeneous nucleation processes are still able to increase ice crystal mass, however, and can artificially inflate ice crystal size and increase sedimentation. This model error has been shared with model developers and identified as an issue to be resolved in future releases of CAM (personal communications, A. Gettelman, 2021) (Gettelman, 2021), and one global correction significantly alters the climate sensitivity of CESM2 (Zhu et al., 2021).

174

175

176

177

178

179

180

181

182

183

184

185

186

To assess the importance of this model mechanism on cloud properties and ice number concentration and size, we disable the ice number limit at mixed-phase temperatures ( $-37^{\circ}\text{C} < T < 0^{\circ}\text{C}$ ) in CAM6-Oslo, restoring heterogeneous ice production as well as secondary ice production through the Hallet-Mossop process, and producing an additional model variation we label as CAM6-OsloIce. To isolate the impact of heterogeneous nucleation, we also cap the ice number tendency variable from secondary ice production in CAM6-OsloIce to avoid strong secondary production in the absence of the ice number limit, describing this implementation in the Supplementary Material. To focus on Arctic clouds, these changes are made only in the Arctic Circle (latitude  $> 66^{\circ}\text{N}$ ). Whereas mixed-phase clouds in CAM6 are strongly (and potentially unrealistically) INP-limited by the ice number limit, CAM6-OsloIce serves as an alternate ensemble end-member representing the assumption that transport and entrainment bring in fresh INPs to replace those that nucleated ice in the previous model time step.

187

188

189

190

191

192

193

194

195

196

197

198

199

200

Using nudged 12-month simulations, we iteratively modify the time scale of the WBF process and the number of aerosols active as INPs in the base models (CAM6-Oslo, CAM6, and CAM6-OsloIce) to minimize root-mean-square error with the SLF metrics. Methodology for parameter tuning ranges and validation of ice crystal concentrations is described in the Supplementary Material. This approach produced four “fitted” models that agree with observations. Table 1 summarizes the three base models and four “fitted” models presented in this work, as well as six ancillary simulations in which single parameters were tuned to the “fitted” values. When the ice limit is in place, large INP multipliers increase ice crystal size and decrease the ice number concentration (CAM6 Fit 4 vs CAM6, CAM6-Oslo vs CAM6-Oslo(1,10)), demonstrating non-physical behavior caused by the model error. Conversely, runs without an ice number limit have smaller ice crystals and higher concentrations than those with the limit in place. Ice crystal size and concentration variables in the constrained runs (Table 1) fall near observed ranges from the M-PACE experiment (Prezzi et al., 2009), preventing us from discarding any of the simulations.

201

## 2.5 Radiative Feedback Calculations

202

203

204

205

206

207

We use surface radiative kernels from Soden et al. (2008) to calculate long- and short-wave cloud feedback parameters. We repeat each simulation from Table 1 with prescribed sea surface temperatures increased by 4K globally to create perturbed runs for the radiative feedback calculations. Because we run atmosphere-only simulations and modify models only poleward of  $66^{\circ}\text{N}$ , feedback parameters are calculated with respect to the temperature change in the Arctic rather than the global mean.

Run name	Model	Ice Number Limit (Secondary Ice Limit)	WBF Multiplier	INP Multiplier	Average Ice Radius at 860 hPa ( $\mu\text{m}$ )	Ice Concentration at 860 hPa ( $\text{m}^{-3}$ )
CAM6-Oslo	NorESM2	Yes (No)	1.0	1.0	151	4120
CAM6	CESM2	Yes (No)	1.0	1.0	165	5550
CAM6-OsloIce	NorESM2	No (Yes)	1.0	1.0	132	15670
CAM6-Oslo Fit 1	NorESM2	Yes (No)	1.25	10.0	163	3870
CAM6-OsloIce Fit 2	NorESM2	No (Yes)	0.5	0.05	124	5410
CAM6-OsloIce Fit 3	NorESM2	No (Yes)	0.2	0.1	112	8600
CAM6 Fit 4	CESM2	Yes (No)	1.0	100	209	5060
CAM6-Olso(1.25,1)	NorESM2	Yes (No)	1.25	1.0	156	3950
CAM6-Olso(1,10)	NorESM2	Yes (No)	1.0	10.0	160	4020
CAM6-OsloIce(0.2,1)	NorESM2	No (Yes)	0.2	1.0	112	23460
CAM6-OsloIce(0.5,1)	NorESM2	No (Yes)	0.5	1.0	123	16540
CAM6-OsloIce(1,0.05)	NorESM2	No (Yes)	1.0	0.05	134	4250
CAM6-OsloIce(1,0.1)	NorESM2	No (Yes)	1.0	0.1	134	4430

**Table 1.** Model run descriptions. Prenni et al. (2009) reported an average INP concentration of  $700\text{m}^{-3}$  and a maximum INP concentration  $6000\text{m}^{-3}$  from the M-PACE experiment.

208

### 3 Results

209

#### 3.1 SLF Metrics

210

211

212

213

214

215

216

217

218

219

220

221

222

223

Figure 1(a) shows the SLF metrics from CALIOP observations and the base models. In the CALIOP retrievals, cloud-top SLF is greater than cloud-bulk SLF values for all isotherms between  $-35^{\circ}\text{C}$  and  $-10^{\circ}\text{C}$ . At  $-20^{\circ}\text{C}$  where this difference is the most pronounced, cloud-top SLF exceeds the cloud-bulk value by nearly a factor of three. All models reproduce the structure of icier cloud interiors, but with varying degrees of quantitative agreement with CALIOP: CAM6-Oslo shows strong agreement across both metrics, CAM6 overestimates SLF in cloud tops, and CAM6-OsloIce underestimates SLF along both the cloud-top and cloud-bulk SLF metrics. The poor performance of CAM6-OsloIce results from a high ice number concentration that allows liquid water to be quickly depleted. Differences in SLF between CAM6-Oslo and CAM6-OsloIce mostly occur at cold isotherms where secondary ice processes are not active, showing that freed heterogeneous nucleation processes are responsible for the cloud changes between these models and that environments with few INPs are necessary for maintaining liquid cloud tops below  $20^{\circ}\text{C}$ . Figure 1(b) shows SLF metrics for CALIOP and the fitted models.

224

225

#### 3.2 Evaluation against CALIOP-GOCCP and CERES-EBAF data products

226

227

228

229

230

231

232

233

234

235

236

Monthly averages of cloud fraction by CALIOP phase designation allow us to identify seasonal trends and biases (Figure 2). We find that fitting to the SLF metrics brings CAM6-Oslo and CAM6-OsloIce models into good agreement with each other, indicating that the effect of removing the limit on ice number can be compensated for with the adjustment of the WBF and INP parameters. In the summer and early fall, the total cloud fraction and the liquid and ice components are consistent across all models, with an overestimation of liquid and total cloud fraction during June and July. Differences between models emerge in the winter and spring months. CAM6-OsloIce, CAM6-Oslo Fit 1, CAM6-Oslo Fit 2, and CAM6 Fit 4 all produce insufficient total cloud fraction during the winter, while CAM6 produces excess total cloud fraction. All models fail to capture the total cloud fraction in the spring, mostly due to insufficient ice cloud fraction.

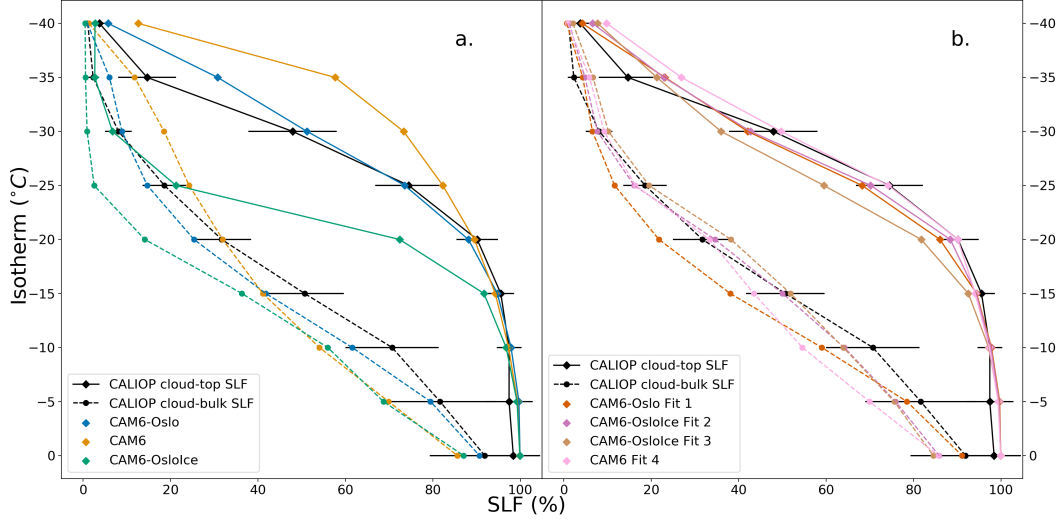


**Figure 1.** Supercooled liquid fraction by isotherm for cloud-top and cloud-bulk metrics for (a) base models and (b) fitted models. Error bars on CALIOP SLF values correspond to one standard deviation. All values represent an area-weighted average from 66°-82°N.

237  
238

Finally, a positive liquid cloud bias in CAM6 persists throughout the year and is especially pronounced during the winter.

239  
240  
241  
242  
243  
244  
245  
246

Annual model biases in Arctic-averaged cloud fraction and CRE with respect to CALIOP-GOCCP and CERES-EBAF (Table S1) follow the results of Figure 2. Notable compensating biases in cloud fraction by phase are present, with CAM6 producing excess liquid cloud and insufficient ice cloud, and CAM6-OsloIce producing excess ice cloud and insufficient liquid cloud. CAM6 Fit 4 shares the ice cloud bias of CAM6 despite having good agreement with the observed SLF metrics because positive biases in mid- and high-level ice clouds are unaffected by the model adjustments. Polar projections of model cloud phase biases (Figure S2) show the spatial features of model cloud phase biases.

247  
248  
249  
250  
251  
252  
253  
254  
255

All simulations have negative shortwave CRE biases between  $-2.9$  and  $-5.1 \text{ Wm}^{-2}$  in the annual mean due to the shared positive cloud fraction bias in the summer. Downwelling shortwave surface flux and CRE biases (Fig. 3(a) and (b)) strongly resemble each other, confirming that clouds are responsible for the shortwave biases. Excessive summer cloudiness is largely independent of mixed-phase processes, since low-level liquid clouds make up roughly two thirds of the total cloud fraction during the summer months in our simulations (Fig. S3). Because the shortwave CRE is similar between model runs, changes in mixed-phase microphysics impact the Arctic mainly through the longwave CRE in the winter and spring.

256  
257  
258  
259  
260  
261  
262  
263  
264  
265

Like the shortwave, the downwelling longwave surface flux and CRE biases (Fig. 3(c) and (d)) are also highly similar. There is strong seasonal variation in the longwave biases, with excess downward flux from clouds in the summer and insufficient downward flux in the winter. The positive summer biases occur when all models produce excess cloud fraction, but the negative wintertime biases occur even in the models that capture both cloud fraction and phase well. CAM6 is the only model to capture the downward flux despite overproducing winter cloud fraction, suggesting biases in cloud height and emission temperature across all simulations. While passive sensors and their corresponding satellite simulators are poorly suited to constrain this behavior, cloud height and opacity variables recently incorporated into the COSP2 Lidar simulator will allow this win-

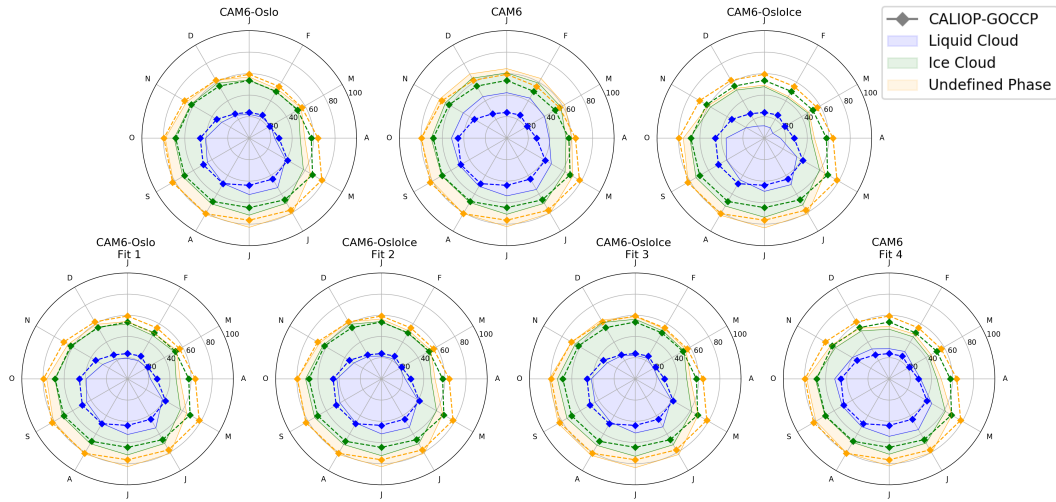


**Figure 2.** Comparison of monthly cloud fraction by phase. Model values are produced by the COSP CALIPSO satellite simulator and observations are from the CALIPSO-GOCCP cloud phase products. The different cloud phase components are stacked on top of each other so that the outermost contour gives the total cloud fraction and compensating phase biases can be easily visualized.

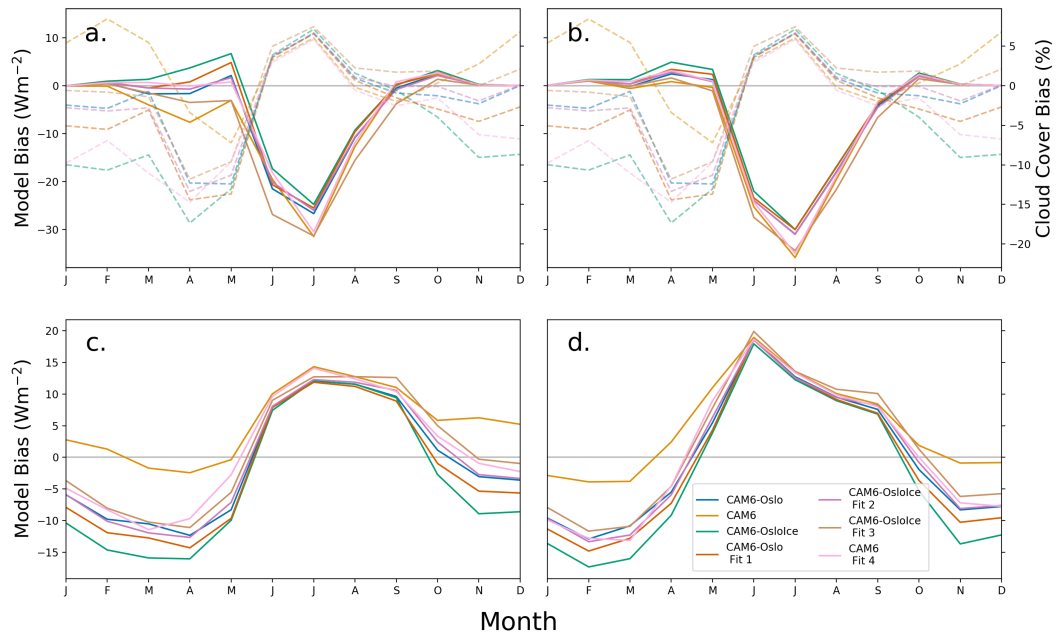


**Figure 3.** Monthly values for: (a) Model bias in shortwave downwelling flux at the surface (solid) and total cloud fraction (dashed), (b) Model bias in surface shortwave cloud radiative effect (solid) and total cloud fraction (dashed), (c) Model bias in longwave downwelling flux at the surface, (d) Model bias in surface longwave cloud radiative effect.

266 tertime bias to be investigated in future versions of CAM (Guzman et al., 2017; A. L. Mor-  
 267 rison et al., 2019).

### 268 3.3 Cloud Radiative Feedbacks

269 Computing cloud radiative feedbacks allows us to assess the relative importance  
 270 of the long- and shortwave cloud feedback processes and to investigate their dependence  
 271 on the present-day cloud state and cloud microphysical properties. Figure 4(a) shows  
 272 the long- and shortwave cloud feedback parameters and the net cloud feedback for each  
 273 model simulation.

274 Differences in present day cloud fraction and phase are greatest in the winter and  
 275 spring, suggesting that mixed-phase processes impact cloud feedbacks most during this  
 276 time. We investigate how low-level (cloud-top pressure > 680 mb) liquid cloud fraction  
 277 changes between the present day and +4K warming simulations (Figure 4(b)) correlate  
 278 with the longwave cloud feedback parameter, finding that the average change in low-level  
 279 liquid cloud fraction from November through April is strongly correlated with the long-  
 280 wave feedback ( $R^2 = 0.92$ ) (Figure 4(c)). Individual correlations by month indicate that  
 281 this pattern is consistent from November through April, whereas no correlation is found  
 282 from May through October (Figure S4).

283 To investigate why different parametrizations give rise to these feedbacks, we pro-  
 284 pose that the slope of the SLF curves in Fig. 1 should determine how quickly liquid clouds  
 285 replace ice clouds during warming. Since the SLF metrics change little in our +4K sim-  
 286 ulations (Fig. S5), cloud phase changes occur because atmospheric warming shifts clouds  
 287 to warmer isotherms where liquid replaces ice. The SLF metrics effectively describe the  
 288 sensitivity of cloud phase to warming, potentially offering a predictor of longwave cloud  
 289 feedback. We approximate this sensitivity as the change in SLF between the -10C and  
 290 -30C isotherms and correlate this value with the LW cloud feedback (Fig. 4(d)). All but  
 291 one model (CAM6 Fit 4) show agreement with the predicted relationship. We hypoth-  
 292 esize that large ice crystal sizes in CAM6 Fit 4 (Table 1) depress ice cloud lifetimes and  
 293 lead to a much larger increase in low-level liquid cloud amount under warming, but leave  
 294 this question open for future work. Excluding CAM6 Fit 4 from our analysis (Fig. 4(d)  
 295 grey lines and text) demonstrates that the SLF metric can effectively predict the LW cloud  
 296 feedback. These results demonstrate that different parametrizations of mixed-phase pro-  
 297 cesses impact Arctic warming by modifying how low-level liquid clouds increase in re-  
 298 sponse to warming.

## 299 4 Discussion and Conclusion

300 We find large differences in thermodynamic phase between cloud tops and interi-  
 301 ors in satellite observations of Arctic mixed-phase clouds, consistent with previous ground-  
 302 based measurements. CAM6-Oslo captures this vertical phase structure better than CAM6,  
 303 suggesting that model aerosol schemes and high cloud parameterizations play an impor-  
 304 tant role in determining cloud phase. We evaluate a significant model error that prevents  
 305 heterogeneous and secondary nucleation processes from creating new ice crystals and find  
 306 that cloud water is significantly reduced when these nucleation processes are able to op-  
 307 erate freely.

308 All models produce insufficient cloud fraction in the spring and excess cloud frac-  
 309 tion in the summer. The summer bias dominates the shortwave impact, leading to a net  
 310 negative annual shortwave flux bias. Longwave flux biases are strongly seasonal, with  
 311 positive summer biases explained by excess summer cloud fraction and negative winter  
 312 biases likely resulting from low-biased cloud emission temperatures. The greatest vari-  
 313 ation between models occurs in the winter and spring, and changes in low-level liquid  
 314 cloud fraction under warming during these seasons are strongly correlated with the long-

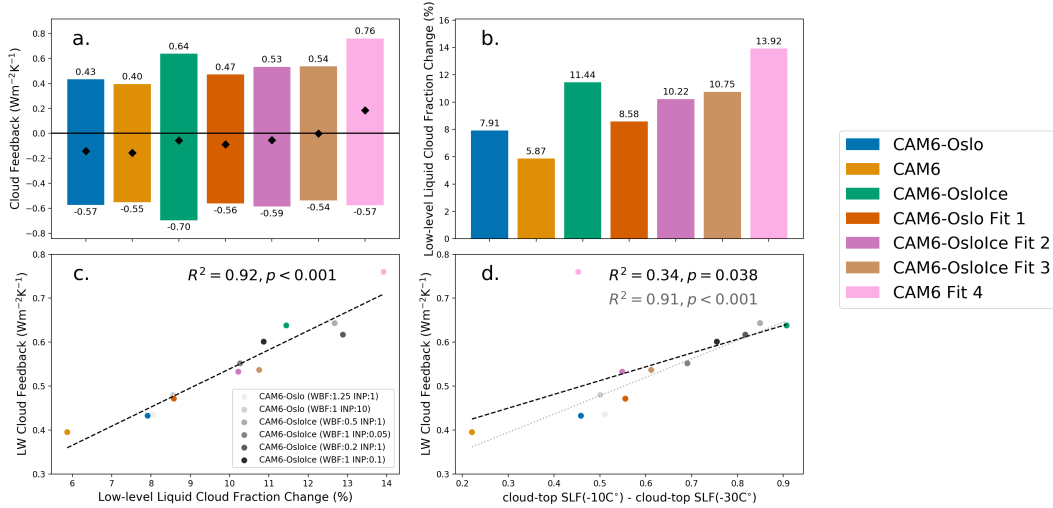


**Figure 4.** a. Arctic-averaged longwave and shortwave cloud feedback. Diamonds denote the net cloud feedback. Kernel calculations do not incorporate surface albedo changes with mean state when calculating shortwave cloud feedback and tend to overestimate the shortwave cooling effect of clouds at high latitudes. b. Arctic-averaged change in low-level liquid cloud fraction between present-day and +4K simulations. c. Longwave cloud feedback as a function of the mean change in low-level liquid cloud fraction from November to April. d. Longwave cloud feedback as a function of the difference in cloud-top SLF between the  $-10^{\circ}C$  and  $-30^{\circ}C$  isotherms. In panel d, grey text and best fit lines represent analysis excluding CAM6 Fit 4.

315 wave cloud feedback parameter. Our results indicate that the parametrization of mixed-  
 316 phase microphysics influences the Arctic climate by modifying how winter and spring  
 317 clouds respond to warming, and that cloud phase observations may constrain this rela-  
 318 tionship. Positive longwave cloud feedback associated with winter cloud fraction increases  
 319 was also observed in fully-coupled simulations of CESM1 (A. L. Morrison et al., 2019),  
 320 raising to question the relative contributions of sea ice loss and simple surface warming  
 321 to these winter feedbacks.

322 Our results demonstrate the need to capture local cloud phase processes in order  
 323 to understand how mixed-phase cloud processes impact Arctic warming. Future stud-  
 324 ies should use multiple atmospheric components, and use fully-coupled models to deter-  
 325 mine whether the proposed constraint is valid in a dynamic climate system.

### Acknowledgments

326 This project has received funding from the European Research Council (ERC) under the  
 327 European Union’s Horizon 2020 research and innovation programme under grant agree-  
 328 ment No 714062 (ERC Starting Grant “C2Phase”). This work was supported by the Eu-  
 329 ropean Research Council (ERC) through Grant StG 758005, and by the Norwegian Re-  
 330 search Council through grant 295046. The computations and simulations were performed  
 331 on resources provided by UNINETT Sigma2 - the National Infrastructure for High Per-  
 332 formance Computing and Data Storage in Norway. JKS acknowledges funding from a  
 333 Fulbright Student Research Grant. JKS also thanks Anne Claire Fouilloux and Inger He-  
 334 lene Karset for technical support and JE Kay for comments.  
 335

336 CALIOP and CERES-EBAF data are available online at the NASA Langley At-  
 337 mospheric Sciences Data Center website (<https://asdc.larc.nasa.gov/>). The CALIOP GOCCP

338  
339  
340

observational data set can be downloaded from <https://climserv.ipsl.polytechnique.fr/cfmip-obs/>. The ERA-Interim reanalysis data can be downloaded freely (<https://www.ecmwf.int/en/forecasts/datasets/datasets/era-interim>).

341

## References

342  
343  
344  
345  
346  
347  
348  
349  
350  
351  
352  
353  
354  
355  
356  
357  
358  
359  
360  
361  
362  
363  
364  
365  
366  
367  
368  
369  
370  
371  
372  
373  
374  
375  
376  
377  
378  
379  
380  
381  
382  
383  
384  
385  
386  
387  
388  
389  
390

- Boucher, O., Randall, D., Artaxo, P., Bretherton, C., Feingold, G., Forster, P., ... Zhang, X. (2013). Clouds and aerosols [Book Section]. In T. Stocker et al. (Eds.), *Climate change 2013: The physical science basis. contribution of working group i to the fifth assessment report of the intergovernmental panel on climate change* (p. 571–658). Cambridge, United Kingdom and New York, NY, USA: Cambridge University Press. Retrieved from [www.climatechange2013.org](http://www.climatechange2013.org) doi: 10.1017/CBO9781107415324.016
- Cesana, G., & Chepfer, H. (2012). How well do climate models simulate cloud vertical structure? a comparison between calipso-goccp satellite observations and cmip5 models. *Geophysical Research Letters*, *39*(20). Retrieved from <https://agupubs.onlinelibrary.wiley.com/doi/abs/10.1029/2012GL053153> doi: 10.1029/2012GL053153
- Cesana, G., Kay, J. E., Chepfer, H., English, J. M., & de Boer, G. (2012). Ubiquitous low-level liquid-containing arctic clouds: New observations and climate model constraints from calipso-goccp. *Geophysical Research Letters*, *39*(20). Retrieved from <https://agupubs.onlinelibrary.wiley.com/doi/abs/10.1029/2012GL053385> doi: 10.1029/2012GL053385
- Chepfer, H., Bony, S., Winker, D., Cesana, G., Dufresne, J. L., Minnis, P., ... Zeng, S. (2010). The gcm-oriented calipso cloud product (calipso-goccp). *Journal of Geophysical Research: Atmospheres*, *115*(D4). Retrieved from <https://agupubs.onlinelibrary.wiley.com/doi/abs/10.1029/2009JD012251> doi: 10.1029/2009JD012251
- Danabasoglu, G., Lamarque, J.-F., Bacmeister, J., Bailey, D. A., DuVivier, A. K., Edwards, J., ... Strand, W. G. (2020). The community earth system model version 2 (cesm2). *Journal of Advances in Modeling Earth Systems*, *12*(2), e2019MS001916. Retrieved from <https://agupubs.onlinelibrary.wiley.com/doi/abs/10.1029/2019MS001916> (e2019MS001916 2019MS001916) doi: 10.1029/2019MS001916
- Dee, D. P., Uppala, S. M., Simmons, A. J., Berrisford, P., Poli, P., Kobayashi, S., ... Vitart, F. (2011). The era-interim reanalysis: configuration and performance of the data assimilation system. *Quarterly Journal of the Royal Meteorological Society*, *137*(656), 553–597. Retrieved from <https://rmets.onlinelibrary.wiley.com/doi/abs/10.1002/qj.828> doi: 10.1002/qj.828
- Eyring, V., Bony, S., Meehl, G. A., Senior, C. A., Stevens, B., Stouffer, R. J., & Taylor, K. E. (2016). Overview of the coupled model intercomparison project phase 6 (cmip6) experimental design and organization. *Geoscientific Model Development*, *9*(5), 1937–1958. Retrieved from <https://www.geosci-model-dev.net/9/1937/2016/> doi: 10.5194/gmd-9-1937-2016
- Feldl, N., Po-Chedley, S., Singh, H. K. A., Hay, S., & Kushner, P. J. (2020, Oct 22). Sea ice and atmospheric circulation shape the high-latitude lapse rate feedback. *npj Climate and Atmospheric Science*, *3*(1), 41. Retrieved from <https://doi.org/10.1038/s41612-020-00146-7> doi: 10.1038/s41612-020-00146-7
- Fridlind, A. M., Ackerman, A. S., McFarquhar, G., Zhang, G., Poellot, M. R., DeMott, P. J., ... Heymsfield, A. J. (2007). Ice properties of single-layer stratocumulus during the mixed-phase arctic cloud experiment: 2. model results. *Journal of Geophysical Research: Atmospheres*, *112*(D24). Retrieved from <https://agupubs.onlinelibrary.wiley.com/doi/abs/10.1029/>

- 391 2007JD008646 doi: 10.1029/2007JD008646
- 392 Fu, S., Deng, X., Shupe, M. D., & Xue, H. (2019). A modelling study of the contin-  
 393 uous ice formation in an autumnal arctic mixed-phase cloud case. *Atmospheric*  
 394 *Research*, 228, 77 - 85. Retrieved from [http://www.sciencedirect.com/](http://www.sciencedirect.com/science/article/pii/S0169809518313905)  
 395 [science/article/pii/S0169809518313905](http://www.sciencedirect.com/science/article/pii/S0169809518313905) doi: [https://doi.org/10.1016/](https://doi.org/10.1016/j.atmosres.2019.05.021)  
 396 [j.atmosres.2019.05.021](https://doi.org/10.1016/j.atmosres.2019.05.021)
- 397 Gettelman, A. (2021). *Issue #20 escomp/pumas*. [https://github.com/ESCOMP/](https://github.com/ESCOMP/PUMAS/issues/20)  
 398 [PUMAS/issues/20](https://github.com/ESCOMP/PUMAS/issues/20). GitHub.
- 399 Goosse, H., Kay, J. E., Armour, K. C., Bodas-Salcedo, A., Chepfer, H., Docquier,  
 400 D., ... Vancoppenolle, M. (2018). Quantifying climate feedbacks in polar re-  
 401 gions. *Nature Communications*, 9(1), 1919. Retrieved from [https://doi.org/](https://doi.org/10.1038/s41467-018-04173-0)  
 402 [10.1038/s41467-018-04173-0](https://doi.org/10.1038/s41467-018-04173-0) doi: 10.1038/s41467-018-04173-0
- 403 Guzman, R., Chepfer, H., Noel, V., Vaillant de Guélis, T., Kay, J. E., Raberanto, P.,  
 404 ... Winker, D. M. (2017). Direct atmosphere opacity observations from calipso  
 405 provide new constraints on cloud-radiation interactions. *Journal of Geophys-*  
 406 *ical Research: Atmospheres*, 122(2), 1066-1085. Retrieved from [https://](https://agupubs.onlinelibrary.wiley.com/doi/abs/10.1002/2016JD025946)  
 407 [agupubs.onlinelibrary.wiley.com/doi/abs/10.1002/2016JD025946](https://agupubs.onlinelibrary.wiley.com/doi/abs/10.1002/2016JD025946) doi:  
 408 <https://doi.org/10.1002/2016JD025946>
- 409 Hobbs, P. V., & Rangno, A. L. (1998). Microstructures of low and middle-  
 410 level clouds over the beaufort sea. *Quarterly Journal of the Royal Me-*  
 411 *teorological Society*, 124(550), 2035-2071. Retrieved from [https://](https://rmets.onlinelibrary.wiley.com/doi/abs/10.1002/qj.49712455012)  
 412 [rmets.onlinelibrary.wiley.com/doi/abs/10.1002/qj.49712455012](https://rmets.onlinelibrary.wiley.com/doi/abs/10.1002/qj.49712455012) doi:  
 413 [10.1002/qj.49712455012](https://doi.org/10.1002/qj.49712455012)
- 414 Hoose, C., Lohmann, U., Bennartz, R., Croft, B., & Lesins, G. (2008). Global sim-  
 415 ulations of aerosol processing in clouds. *Atmospheric Chemistry and Physics*,  
 416 8(23), 6939–6963. Retrieved from [https://www.atmos-chem-phys.net/8/](https://www.atmos-chem-phys.net/8/6939/2008/)  
 417 [6939/2008/](https://www.atmos-chem-phys.net/8/6939/2008/) doi: 10.5194/acp-8-6939-2008
- 418 Huang, Y., Dong, X., Kay, J. E., Xi, B., & McIlhattan, E. A. (2021, May 01). The  
 419 climate response to increased cloud liquid water over the arctic in cesm1:  
 420 a sensitivity study of wegener–bergeron–findeisen process. *Climate Dy-*  
 421 *namics*, 56(9), 3373-3394. Retrieved from [https://doi.org/10.1007/](https://doi.org/10.1007/s00382-021-05648-5)  
 422 [s00382-021-05648-5](https://doi.org/10.1007/s00382-021-05648-5) doi: 10.1007/s00382-021-05648-5
- 423 Jiang, H., Cotton, W. R., Pinto, J. O., Curry, J. A., & Weissbluth, M. J. (2000).  
 424 Cloud resolving simulations of mixed-phase arctic stratus observed during  
 425 base: Sensitivity to concentration of ice crystals and large-scale heat and mois-  
 426 ture advection. *Journal of the Atmospheric Sciences*, 57(13), 2105-2117. Re-  
 427 trieved from [https://doi.org/10.1175/1520-0469\(2000\)057<2105:CRSOMP>](https://doi.org/10.1175/1520-0469(2000)057<2105:CRSOMP>2.0.CO;2)  
 428 [2.0.CO;2](https://doi.org/10.1175/1520-0469(2000)057<2105:CRSOMP>2.0.CO;2) doi: 10.1175/1520-0469(2000)057<2105:CRSOMP>2.0.CO;2
- 429 Kato, S., Rose, F. G., Rutan, D. A., Thorsen, T. J., Loeb, N. G., Doelling, D. R., ...  
 430 Ham, S.-H. (01 Jun. 2018). Surface irradiances of edition 4.0 clouds and the  
 431 earth’s radiant energy system (ceres) energy balanced and filled (ebaf) data  
 432 product. *Journal of Climate*, 31(11), 4501 - 4527. Retrieved from [https://](https://journals.ametsoc.org/view/journals/clim/31/11/jcli-d-17-0523.1.xml)  
 433 [journals.ametsoc.org/view/journals/clim/31/11/jcli-d-17-0523.1.xml](https://journals.ametsoc.org/view/journals/clim/31/11/jcli-d-17-0523.1.xml)  
 434 doi: 10.1175/JCLI-D-17-0523.1
- 435 Kay, J. E., L’Ecuyer, T., Chepfer, H., Loeb, N., Morrison, A., & Cesana, G. (2016).  
 436 Recent advances in arctic cloud and climate research. *Current Climate Change*  
 437 *Reports*, 2(4), 159–169.
- 438 Kirkevåg, A., Grini, A., Olivie, D., Seland, Ø., Alterskjær, K., Hummel, M., ...  
 439 Iversen, T. (2018). A production-tagged aerosol module for earth system mod-  
 440 els, osloaero5.3 – extensions and updates for cam5.3-oslo. *Geoscientific Model*  
 441 *Development*, 11(10), 3945–3982. Retrieved from [https://gmd.copernicus](https://gmd.copernicus.org/articles/11/3945/2018/)  
 442 [.org/articles/11/3945/2018/](https://gmd.copernicus.org/articles/11/3945/2018/) doi: 10.5194/gmd-11-3945-2018
- 443 Komurcu, M., Storelvmo, T., Tan, I., Lohmann, U., Yun, Y., Penner, J. E., ...  
 444 Takemura, T. (2014). Intercomparison of the cloud water phase among global  
 445 climate models. *Journal of Geophysical Research: Atmospheres*, 119(6), 3372-

- 446 3400. Retrieved from [https://agupubs.onlinelibrary.wiley.com/doi/abs/](https://agupubs.onlinelibrary.wiley.com/doi/abs/10.1002/2013JD021119)  
447 10.1002/2013JD021119 doi: 10.1002/2013JD021119
- 448 Korolev, A. (2007). Limitations of the wegener–bergeron–findeisen mechanism in the  
449 evolution of mixed-phase clouds. *Journal of the Atmospheric Sciences*, *64*(9),  
450 3372–3375. Retrieved from <https://doi.org/10.1175/JAS4035.1> doi: 10  
451 .1175/JAS4035.1
- 452 Lenaerts, J. T. M., Gettelman, A., Van Tricht, K., van Kampenhout, L., & Miller,  
453 N. B. (2020). Impact of cloud physics on the greenland ice sheet near-surface  
454 climate: A study with the community atmosphere model. *Journal of Geophys-  
455 ical Research: Atmospheres*, *125*(7), e2019JD031470. Retrieved from [https://](https://agupubs.onlinelibrary.wiley.com/doi/abs/10.1029/2019JD031470)  
456 [agupubs.onlinelibrary.wiley.com/doi/abs/10.1029/2019JD031470](https://agupubs.onlinelibrary.wiley.com/doi/abs/10.1029/2019JD031470)  
457 (e2019JD031470 10.1029/2019JD031470) doi: 10.1029/2019JD031470
- 458 Lenaerts, J. T. M., Van Tricht, K., Lhermitte, S., & L’Ecuyer, T. S. (2017). Polar  
459 clouds and radiation in satellite observations, reanalyses, and climate models.  
460 *Geophysical Research Letters*, *44*(7), 3355–3364. Retrieved from [https://](https://agupubs.onlinelibrary.wiley.com/doi/abs/10.1002/2016GL072242)  
461 [agupubs.onlinelibrary.wiley.com/doi/abs/10.1002/2016GL072242](https://agupubs.onlinelibrary.wiley.com/doi/abs/10.1002/2016GL072242) doi:  
462 <https://doi.org/10.1002/2016GL072242>
- 463 Liu, X., Ma, P.-L., Wang, H., Tilmes, S., Singh, B., Easter, R. C., ... Rasch,  
464 P. J. (2016). Description and evaluation of a new four-mode version of  
465 the modal aerosol module (mam4) within version 5.3 of the community at-  
466 mosphere model. *Geoscientific Model Development*, *9*(2), 505–522. Re-  
467 trieved from <https://gmd.copernicus.org/articles/9/505/2016/> doi:  
468 10.5194/gmd-9-505-2016
- 469 Matus, A. V., & L’Ecuyer, T. S. (2017). The role of cloud phase in earth’s radiation  
470 budget. *Journal of Geophysical Research: Atmospheres*, *122*(5), 2559–2578.  
471 Retrieved from [https://agupubs.onlinelibrary.wiley.com/doi/abs/](https://agupubs.onlinelibrary.wiley.com/doi/abs/10.1002/2016JD025951)  
472 10.1002/2016JD025951 doi: 10.1002/2016JD025951
- 473 Mauritsen, T., Stevens, B., Roeckner, E., Crueger, T., Esch, M., Giorgetta, M.,  
474 ... Tomassini, L. (2012). Tuning the climate of a global model. *Journal*  
475 *of Advances in Modeling Earth Systems*, *4*(3). Retrieved from [https://](https://agupubs.onlinelibrary.wiley.com/doi/abs/10.1029/2012MS000154)  
476 [agupubs.onlinelibrary.wiley.com/doi/abs/10.1029/2012MS000154](https://agupubs.onlinelibrary.wiley.com/doi/abs/10.1029/2012MS000154) doi:  
477 <https://doi.org/10.1029/2012MS000154>
- 478 McIlhatten, E. A., L’Ecuyer, T. S., & Miller, N. B. (2017, June 15). Obser-  
479 vational evidence linking arctic supercooled liquid cloud biases in cesm  
480 to snowfall processes. *Journal of Climate*, *30*(12), 4477–4495. doi:  
481 10.1175/JCLI-D-16-0666.1
- 482 Mitchell, J. F. B., Senior, C. A., & Ingram, W. J. (1989, Sep 01). CO<sub>2</sub> and climate:  
483 a missing feedback? *Nature*, *341*(6238), 132–134. Retrieved from [https://doi](https://doi.org/10.1038/341132a0)  
484 [.org/10.1038/341132a0](https://doi.org/10.1038/341132a0) doi: 10.1038/341132a0
- 485 Morrison, A. L., Kay, J. E., Chepfer, H., Guzman, R., & Yettella, V. (2018). Iso-  
486 lating the liquid cloud response to recent arctic sea ice variability using space-  
487 borne lidar observations. *Journal of Geophysical Research: Atmospheres*,  
488 *123*(1), 473–490. Retrieved from [https://agupubs.onlinelibrary.wiley](https://agupubs.onlinelibrary.wiley.com/doi/abs/10.1002/2017JD027248)  
489 [.com/doi/abs/10.1002/2017JD027248](https://agupubs.onlinelibrary.wiley.com/doi/abs/10.1002/2017JD027248) doi: 10.1002/2017JD027248
- 490 Morrison, A. L., Kay, J. E., Frey, W. R., Chepfer, H., & Guzman, R. (2019). Cloud  
491 response to arctic sea ice loss and implications for future feedback in the cesm1  
492 climate model. *Journal of Geophysical Research: Atmospheres*, *124*(2), 1003-  
493 1020. Retrieved from [https://agupubs.onlinelibrary.wiley.com/doi/abs/](https://agupubs.onlinelibrary.wiley.com/doi/abs/10.1029/2018JD029142)  
494 10.1029/2018JD029142 doi: <https://doi.org/10.1029/2018JD029142>
- 495 Morrison, H., de Boer, G., Feingold, G., Harrington, J., Shupe, M. D., & Sulia, K.  
496 (2012). Resilience of persistent arctic mixed-phase clouds. *Nature Geoscience*,  
497 *5*(1), 11–17. Retrieved from <https://doi.org/10.1038/ngeo1332> doi:  
498 10.1038/ngeo1332
- 499 Morrison, H., & Gettelman, A. (2008). A new two-moment bulk stratiform cloud  
500 microphysics scheme in the community atmosphere model, version 3 (cam3).

- 501 part i: Description and numerical tests. *Journal of Climate*, 21(15), 3642-  
 502 3659. Retrieved from <https://doi.org/10.1175/2008JCLI2105.1> doi:  
 503 10.1175/2008JCLI2105.1
- 504 Pithan, F., & Mauritsen, T. (2014, Mar 01). Arctic amplification dominated by tem-  
 505 perature feedbacks in contemporary climate models. *Nature Geoscience*, 7(3),  
 506 181-184. Retrieved from <https://doi.org/10.1038/ngeo2071> doi: 10.1038/  
 507 ngeo2071
- 508 Prenni, A. J., Demott, P. J., Rogers, D. C., Kreidenweis, S. M., Mcfarquhar,  
 509 G. M., Zhang, G., & Poellot, M. R. (2009). Ice nuclei characteristics from  
 510 m-pace and their relation to ice formation in clouds. *Tellus B: Chemi-  
 511 cal and Physical Meteorology*, 61(2), 436-448. Retrieved from [https://  
 512 www.tandfonline.com/doi/abs/10.1111/j.1600-0889.2008.00415.x](https://www.tandfonline.com/doi/abs/10.1111/j.1600-0889.2008.00415.x) doi:  
 513 10.1111/j.1600-0889.2008.00415.x
- 514 Seland, Ø., Bentsen, M., Seland Graff, L., Oliv  , D., Toniazzo, T., Gjermund-  
 515 sen, A., . . . Schulz, M. (2020). The norwegian earth system model,  
 516 noresm2 – evaluation of thecmip6 deck and historical simulations. *Geo-  
 517 scientific Model Development Discussions*, 2020, 1–68. Retrieved from  
 518 <https://www.geosci-model-dev-discuss.net/gmd-2019-378/> doi:  
 519 10.5194/gmd-2019-378
- 520 Shupe, M. D., & Intrieri, J. M. (2004). Cloud radiative forcing of the arctic surface:  
 521 The influence of cloud properties, surface albedo, and solar zenith angle. *Jour-  
 522 nal of Climate*, 17(3), 616-628. Retrieved from [https://doi.org/10.1175/  
 523 1520-0442\(2004\)017<0616:CRFOTA>2.0.CO;2](https://doi.org/10.1175/1520-0442(2004)017<0616:CRFOTA>2.0.CO;2) doi: 10.1175/1520-0442(2004)  
 524 017(0616:CRFOTA)2.0.CO;2
- 525 Soden, B. J., Held, I. M., Colman, R., Shell, K. M., Kiehl, J. T., & Shields, C. A.  
 526 (2008). Quantifying climate feedbacks using radiative kernels. *Jour-  
 527 nal of Climate*, 21(14), 3504 - 3520. Retrieved from [https://journals  
 528 .ametsoc.org/view/journals/clim/21/14/2007jcli2110.1.xml](https://journals.ametsoc.org/view/journals/clim/21/14/2007jcli2110.1.xml) doi:  
 529 10.1175/2007JCLI2110.1
- 530 Swales, D. J., Pincus, R., & Bodas-Salcedo, A. (2018). The cloud feedback model  
 531 intercomparison project observational simulator package: Version 2. *Geosci-  
 532 tific Model Development*, 11(1), 77–81. Retrieved from [https://www.geosci-  
 533 -model-dev.net/11/77/2018/](https://www.geosci-model-dev.net/11/77/2018/) doi: 10.5194/gmd-11-77-2018
- 534 Tan, I., & Storelvmo, T. (2016). Sensitivity study on the influence of cloud  
 535 microphysical parameters on mixed-phase cloud thermodynamic phase  
 536 partitioning in cam5. *Journal of the Atmospheric Sciences*, 73(2), 709-  
 537 728. Retrieved from <https://doi.org/10.1175/JAS-D-15-0152.1> doi:  
 538 10.1175/JAS-D-15-0152.1
- 539 Tan, I., & Storelvmo, T. (2019). Evidence of strong contributions from mixed-phase  
 540 clouds to arctic climate change. *Geophysical Research Letters*, 46(5), 2894-  
 541 2902. Retrieved from [https://agupubs.onlinelibrary.wiley.com/doi/abs/  
 542 10.1029/2018GL081871](https://agupubs.onlinelibrary.wiley.com/doi/abs/10.1029/2018GL081871) doi: 10.1029/2018GL081871
- 543 Taylor, K. E., Stouffer, R. J., & Meehl, G. A. (2012). An overview of cmip5 and  
 544 the experiment design. *Bulletin of the American Meteorological Society*, 93(4),  
 545 485-498. Retrieved from <https://doi.org/10.1175/BAMS-D-11-00094.1> doi:  
 546 10.1175/BAMS-D-11-00094.1
- 547 Winker, D. M., Vaughan, M. A., Omar, A., Hu, Y., Powell, K. A., Liu, Z., . . .  
 548 Young, S. A. (2009). Overview of the calipso mission and calip data pro-  
 549 cessing algorithms. *Journal of Atmospheric and Oceanic Technology*, 26(11),  
 550 2310-2323. Retrieved from <https://doi.org/10.1175/2009JTECHA1281.1>  
 551 doi: 10.1175/2009JTECHA1281.1
- 552 Zelinka, M. D., Myers, T. A., McCoy, D. T., Po-Chedley, S., Caldwell, P. M.,  
 553 Ceppi, P., . . . Taylor, K. E. (2020). Causes of higher climate sensitivity  
 554 in cmip6 models. *Geophysical Research Letters*, 47(1), e2019GL085782.  
 555 Retrieved from <https://agupubs.onlinelibrary.wiley.com/doi/abs/>

556 10.1029/2019GL085782 (e2019GL085782 10.1029/2019GL085782) doi:  
557 10.1029/2019GL085782  
558 Zhu, J., Otto-Bliesner, B. L., Brady, E. C., Poulsen, C., Shaw, J. K., & Kay, J. E.  
559 (2021). Lgm paleoclimate constraints inform cloud parameterizations and equi-  
560 librium climate sensitivity in cesm2. *Earth and Space Science Open Archive*,  
561 49. Retrieved from <https://doi.org/10.1002/essoar.10507790.1> doi:  
562 10.1002/essoar.10507790.1

# Supporting Information for ”Using satellite observations to evaluate model microphysical representation of Arctic mixed-phase clouds”

J. K. Shaw<sup>1</sup> \*, Z. S. McGraw<sup>1</sup> †, O. Bruno<sup>2</sup>, T. Storelvmo<sup>1,3</sup>, and S. Hofer<sup>1</sup>

<sup>1</sup>Department of Geosciences, University of Oslo, Oslo, Norway

<sup>2</sup>Karlsruhe Institute of Technology, Institute of Meteorology and Climate Research

<sup>3</sup>School of Business, Nord University, Bodø, Norway

## Contents of this file

1. Text S1 - S5

2. Table S1

---

J. Shaw (jonah.shaw@colorado.edu)

\*Now at Department of Atmospheric and  
Oceanic Sciences, University of Colorado,  
Boulder, Colorado, USA

†Now at Department of Applied Physics  
and Applied Mathematics, Columbia  
University and NASA Goddard Institute for  
Space Studies

### 3. Figures S1 - S5

**Text S1. Validation of cloud-bulk SLF metric.** We use new cloud products (Guzman et al., 2017) to study the CALIOP's ability to sample Arctic clouds (Fig. S1). On the annual mean, opaque clouds make up 56% of cloudy scenes and are sampled through an average depth of 1.17km. While more opaque clouds are present in the summer and fall, the sampling depth never falls below 1km, indicating that the cloud-bulk metric samples a distinct thermodynamic regime below the supercooled liquid layer for all seasons.

**Text S2. Calculation of observed and modelled SLF metrics.** Observed SLF is calculated as the ratio of the number of liquid cloud top pixels to the sum of ice plus liquid cloud top pixels following the methods of Bruno, Hoose, Storelvmo, Coopman, and Stengel (2021). Modelled SLF is calculated as the ratio of cloud liquid surface area density to the sum of liquid and ice surface area densities using the methods of Tan, Storelvmo, and Zelinka (2016). Observations are binned into  $1^\circ \times 1^\circ$  gridcells for comparison with model output. Improved comparability of observed and modelled SLF metrics would require the creation of additional GOCCP and COSP2 output fields.

**Text S3. Description of limit on secondary ice nucleation.** The ice number tendency variable from secondary nucleation processes ("nsacwi") is limited to  $10^6 \text{kg}^{-1}$  per microphysics timestep (5 minutes) if it exceeds this value after the Hallet-Mossop secondary ice scheme runs. We only set a cap on the number production, which otherwise would have no limit, unlike the mass term that is subject to cloud mass conservation. We choose a very high cap in order to prevent errors from re-implementing the Hallet-Mossop parameterization that was effectively removed from the model due to the ice number error. Sensitivity tests without the secondary ice limit showed negligible changes in SLF,

confirming the dominant contribution of ice from heterogeneous processes when the model error is removed.

**Text S4. Tuning Methods.** The rate of ice and snow growth via the WBF process is highly-dependent on in-cloud conditions (updraft speed, concentration of cloud droplets and ice crystals) (Korolev, 2007). Previous studies reduced the efficiency of the WBF process in CAM5 by factors up to 10 to increase cloud liquid (Tan et al., 2016; Huang et al., 2021). We perform an identical modification in CAM6 to modify the WBF rate.

Tan et al. (2016) also modified the fraction of dust aerosols active as ice nuclei, presenting results with multipliers of 0.79 and 0.19. We perform a similar modification by scaling the aerosol concentration variables that are fed into the Hoose heterogeneous ice nucleation scheme ("total\_aer\_num", "coated\_aer\_num", "uncoated\_aer\_num", "total\_interstitial\_aer\_num", "total\_cloudborne\_aer\_num") (Hoose et al., 2008). We initially tested WBF rate multipliers between 0.1 and 10, and INP multipliers between 0.01 and 100. WBF multipliers significantly greater than 1 have not been previously used, and we found that values greater than 2 significantly reduced SLF in both metrics. INP multipliers varying over several orders of magnitude are reasonable, since observations exhibit high variability (DeMott et al., 2010) and our model variants respond differently to changes in these parameters.

**Text S5. Evaluation of Ice Crystal Concentrations.** We wish to evaluate whether our simulations have ice crystal concentrations that are reasonably consistent with observations. Observations of INP concentrations from the M-PACE field experiment (Prenni et al., 2009) provide one of the few records of INP concentrations for low- and mid-level Arctic clouds. We note that while there is not necessarily a 1-to-1 relationship between

INP concentrations and ice crystal number concentration, INP concentrations are a useful indication of what ice crystal number concentrations are reasonable. Prenni et al. (2009) report a mean INP concentration of  $0.7\text{L}^{-1}$  and a maximum INP concentration of  $60\text{L}^{-1}$ . Prenni et al. (2009) note that INPs greater than  $1.5\mu\text{m}$  were not measured, excluding some INPs from analysis. Ice crystal concentration in our fitted model simulations fall near the values reported by Prenni et al. (2009), indicating that ice crystals are reasonably reproduced by the models. The authors note that a strict comparison between our model output and observations from M-PACE would require specific knowledge of the cloud conditions during the field experiment and targeted modelling experiments beyond the scope of this study.

## References

- Bruno, O., Hoose, C., Storelvmo, T., Coopman, Q., & Stengel, M. (2021). Exploring the cloud top phase partitioning in different cloud types using active and passive satellite sensors. *Geophysical Research Letters*, *48*(2), e2020GL089863. Retrieved from <https://agupubs.onlinelibrary.wiley.com/doi/abs/10.1029/2020GL089863> (e2020GL089863 2020GL089863) doi: <https://doi.org/10.1029/2020GL089863>
- DeMott, P. J., Prenni, A. J., Liu, X., Kreidenweis, S. M., Petters, M. D., Twohy, C. H., ... Rogers, D. C. (2010). Predicting global atmospheric ice nuclei distributions and their impacts on climate. *Proceedings of the National Academy of Sciences*, *107*(25), 11217–11222. Retrieved from <https://www.pnas.org/content/107/25/11217> doi: 10.1073/pnas.0910818107
- Guzman, R., Chepfer, H., Noel, V., Vaillant de Guélis, T., Kay, J. E., Raberanto,

- P., ... Winker, D. M. (2017). Direct atmosphere opacity observations from calipso provide new constraints on cloud-radiation interactions. *Journal of Geophysical Research: Atmospheres*, *122*(2), 1066-1085. Retrieved from <https://agupubs.onlinelibrary.wiley.com/doi/abs/10.1002/2016JD025946> doi: <https://doi.org/10.1002/2016JD025946>
- Hoose, C., Lohmann, U., Bennartz, R., Croft, B., & Lesins, G. (2008). Global simulations of aerosol processing in clouds. *Atmospheric Chemistry and Physics*, *8*(23), 6939–6963. Retrieved from <https://www.atmos-chem-phys.net/8/6939/2008/> doi: 10.5194/acp-8-6939-2008
- Huang, Y., Dong, X., Kay, J. E., Xi, B., & McIlhattan, E. A. (2021, May 01). The climate response to increased cloud liquid water over the arctic in cesm1: a sensitivity study of wegener–bergeron–findeisen process. *Climate Dynamics*, *56*(9), 3373-3394. Retrieved from <https://doi.org/10.1007/s00382-021-05648-5> doi: 10.1007/s00382-021-05648-5
- Korolev, A. (2007). Limitations of the wegener–bergeron–findeisen mechanism in the evolution of mixed-phase clouds. *Journal of the Atmospheric Sciences*, *64*(9), 3372-3375. Retrieved from <https://doi.org/10.1175/JAS4035.1> doi: 10.1175/JAS4035.1
- Prenni, A. J., Demott, P. J., Rogers, D. C., Kreidenweis, S. M., Mcfarquhar, G. M., Zhang, G., & Poellot, M. R. (2009). Ice nuclei characteristics from m-pace and their relation to ice formation in clouds. *Tellus B: Chemical and Physical Meteorology*, *61*(2), 436-448. Retrieved from <https://www.tandfonline.com/doi/abs/10.1111/j.1600-0889.2008.00415.x> doi: 10.1111/j.1600-0889.2008.00415.x

Tan, I., Storelvmo, T., & Zelinka, M. D. (2016). Observational constraints on mixed-phase clouds imply higher climate sensitivity. *Science*, *352*(6282), 224–227. Retrieved from <https://science.sciencemag.org/content/352/6282/224> doi: 10.1126/science.aad5300

Run name	Total Cloud Bias (%)	Liquid Cloud Bias (%)	Ice Cloud Bias (%)	Undefined Cloud Bias (%)	Shortwave CRE Bias (W/m <sup>2</sup> )	Longwave CRE Bias (W/m <sup>2</sup> )
CAM6-Oslo	-2.0	-0.7	0.7	-1.8	-3.5	-0.1
CAM6	2.1	11.2	-7.9	-0.8	-4.0	-0.8
CAM6-OsloIce	-5.8	-8.2	6.1	-3.4	-2.9	0.3
CAM6-Oslo Fit 1	-3.6	-2.2	1.1	-2.2	-3.0	-0.6
CAM6-OsloIce Fit 2	-2.0	-0.9	1.6	-2.4	-3.7	0.4
CAM6-OsloIce Fit 3	-0.3	-1.3	3.6	-2.3	-5.1	1.8
CAM6 Fit 4	-5.1	5.4	-8.1	-2.0	-3.3	-1.9
CAM6-Olso(1.25,1)	-2.8	-1.5	1.0	-2.0	-3.1	-0.4
CAM6-Olso(1,10)	-2.8	-1.4	0.8	-1.9	-3.4	-0.3
CAM6-OsloIce(0.2,1)	-2.1	-6.4	7.6	-3.0	-5.5	2.5
CAM6-OsloIce(0.5,1)	-4.2	-6.8	6.1	-3.1	-4.1	1.2
CAM6-OsloIce(1,0.05)	-4.3	-3.3	2.1	-2.8	-2.2	-0.7
CAM6-OsloIce(1,0.1)	-4.9	-4.3	2.6	-2.9	-2.2	-0.8

**Table S1.** Annual model cloud biases for the region 66°N-82°N. Cloud cover biases are calculated relative to CALIOP GOCCP observations. Surface cloud radiative effect (CRE) biases are calculated relative to CERES-EBAF observations using a positive downward sign convention.

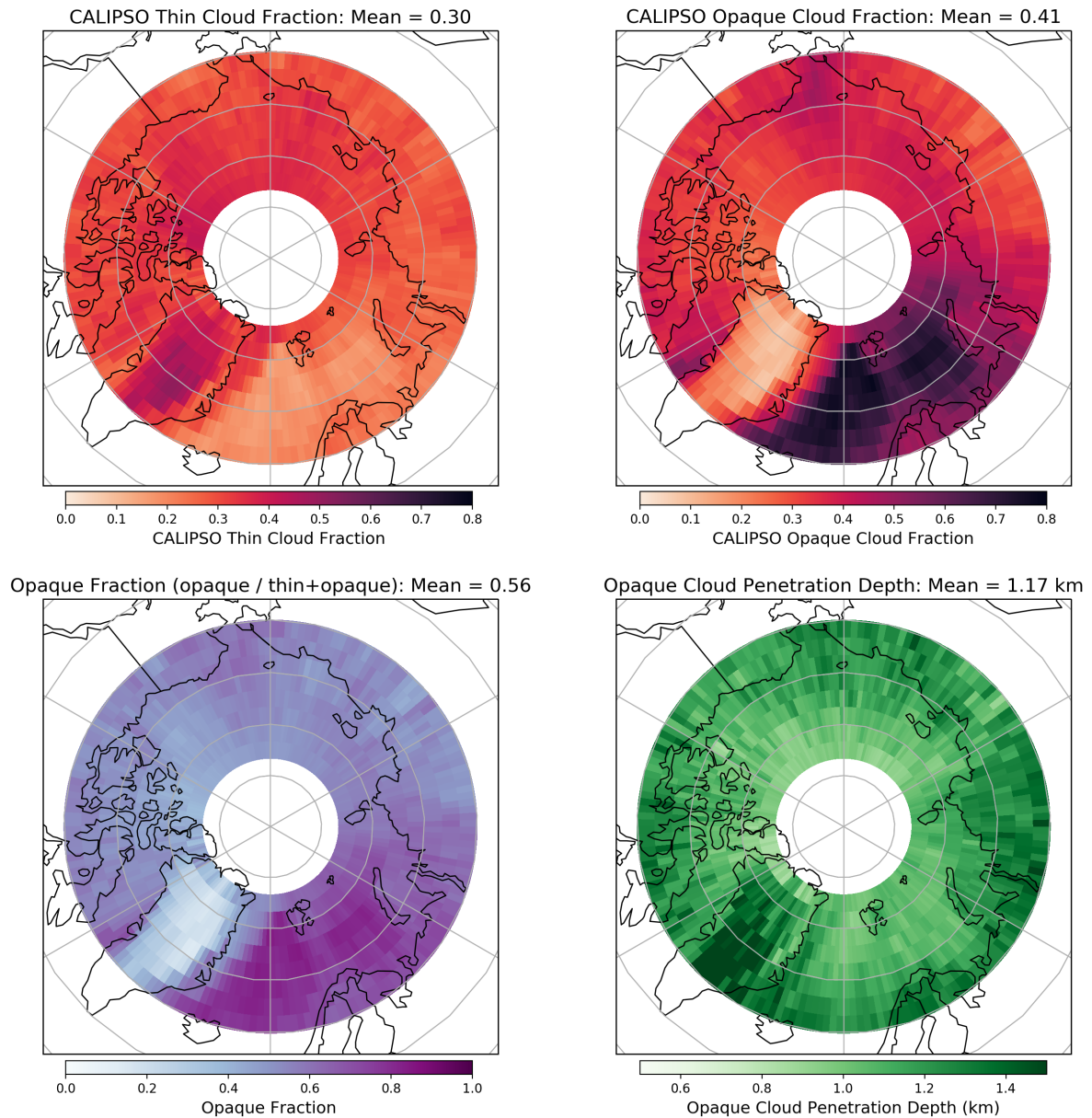


**Figure S1.** Arctic maps (66–90°N) of a) Thin Cloud Fraction from CALIOP, b) Opaque Cloud Fraction from CALIOP, c) Opaque Fraction (opaque cloud fraction / total cloud fraction) from CALIOP, and d) Cloud sampling depth from CALIOP. Cloud sampling depth is computed as the difference between cloud height and opacity height using cloud opacity products developed in Guzman et al. (2017). Mean values are computed as the area-weighted average of the plotted region.

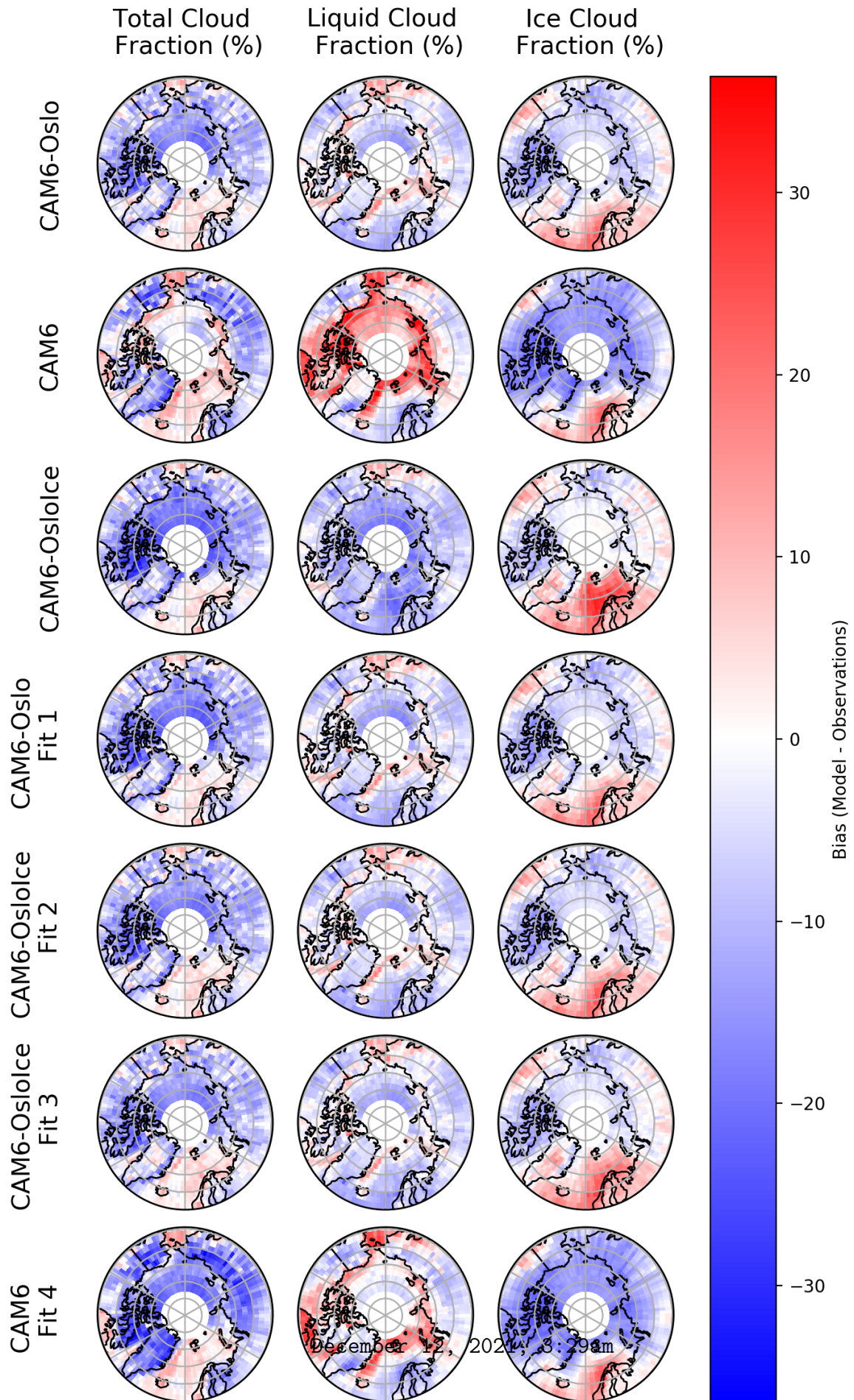
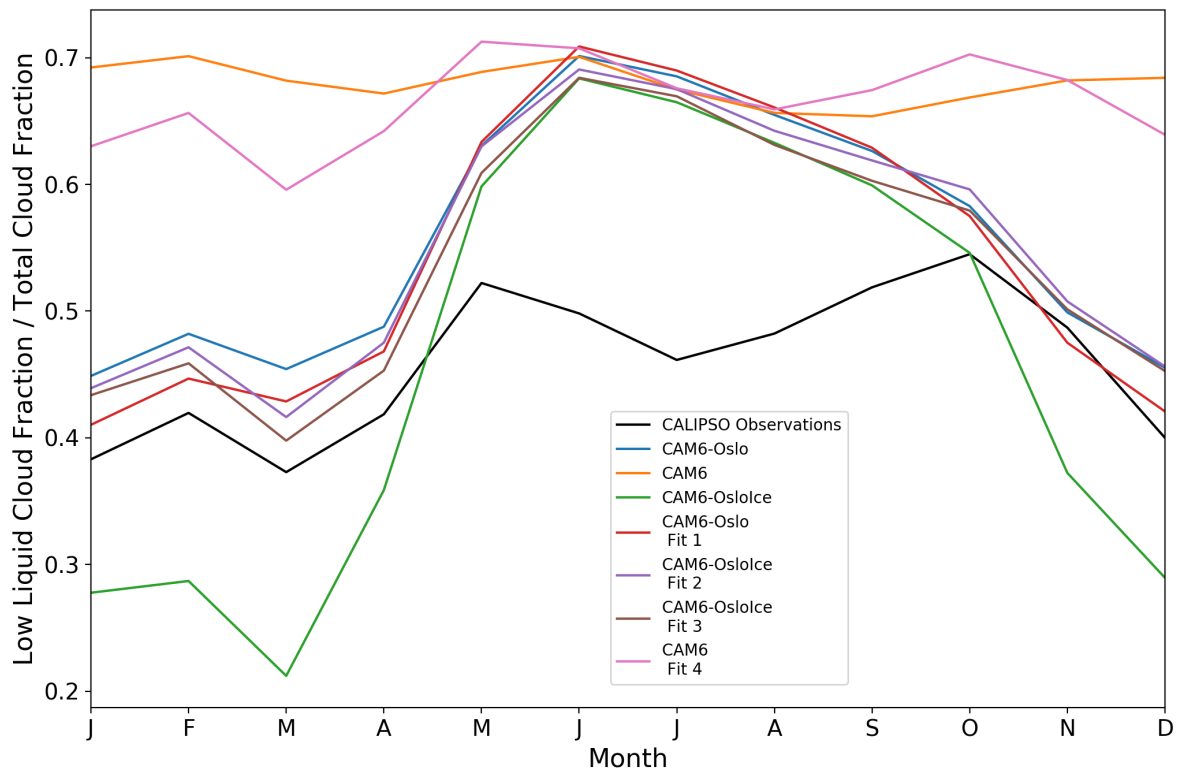
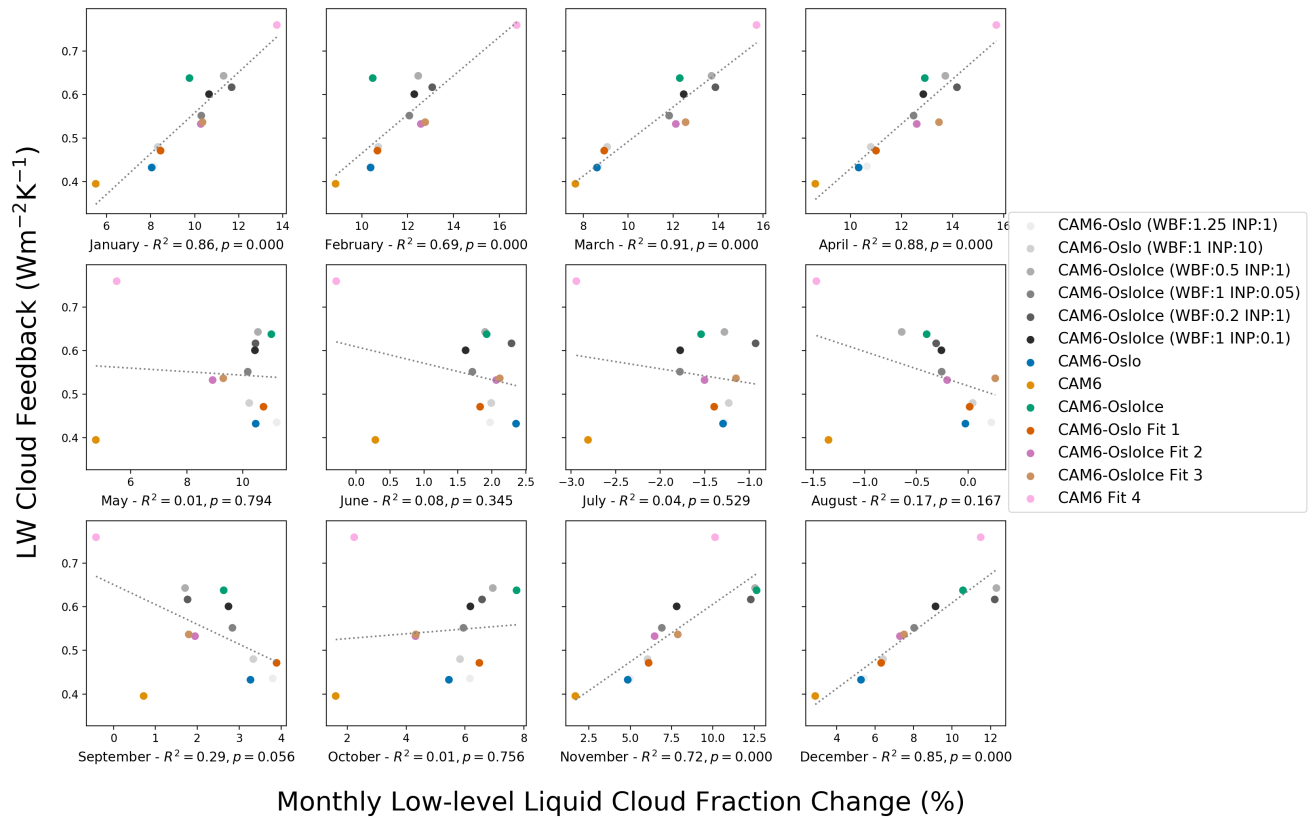


Figure S2. North Pole maps (60–82°N) of cloud cover bias by CALIOP phase designation.



**Figure S3.** Monthly values for the fraction of total cloud made up of low-level liquid phase clouds (low-level liquid cloud fraction / total cloud fraction). Observations are taken from the CALIOP GOCCP cloud product. Model values are computed using variables from the COSP satellite simulator package.



**Figure S4.** Longwave cloud feedback as a function of the change in low-level liquid cloud fraction between present day and +4K simulations by month.

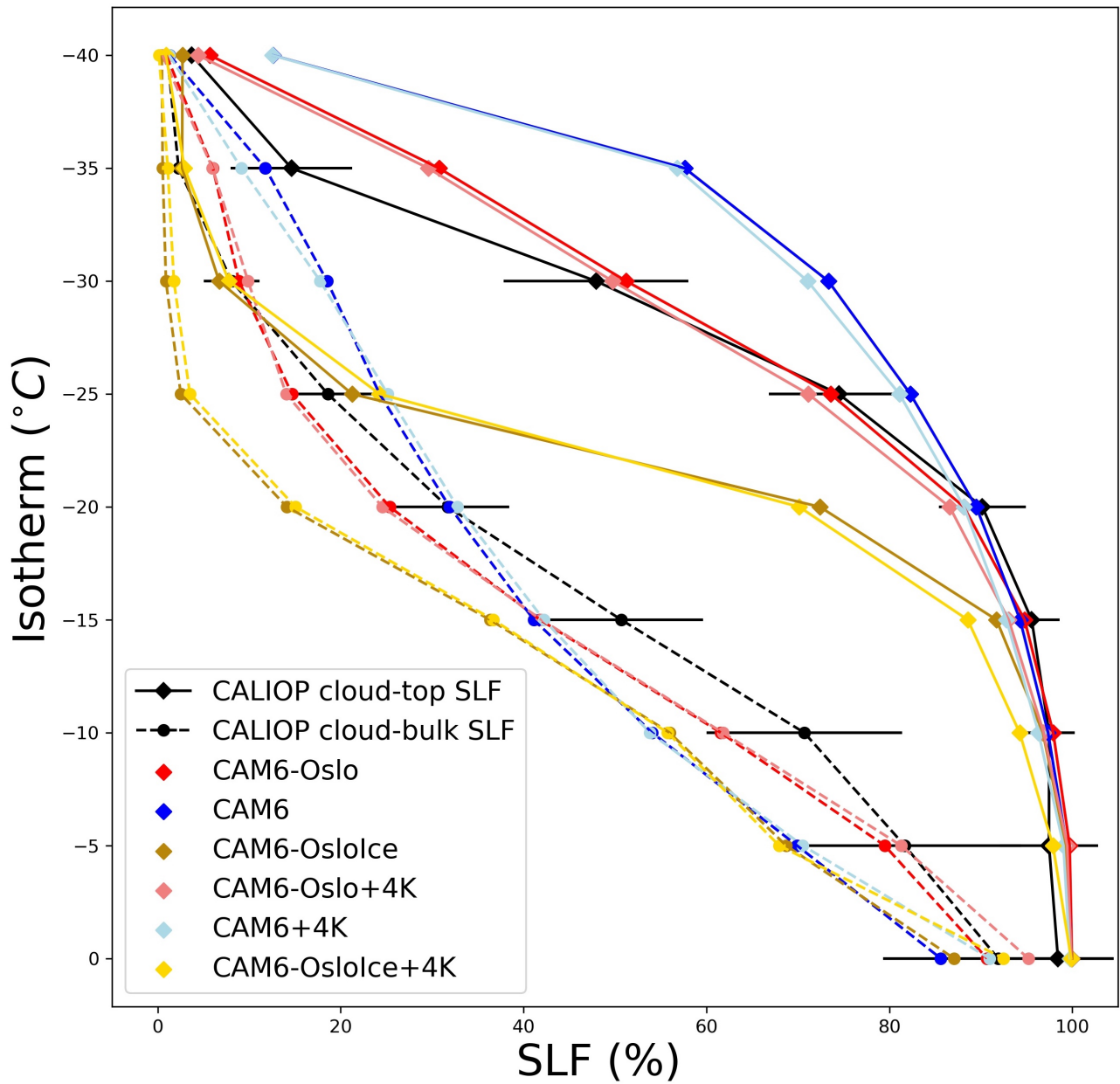


**Figure S5.** Supercooled liquid fraction by isotherm for cloud-top and cloud-bulk metrics for present-day base model simulations and +4K base model simulations. Error bars on CALIOP SLF values correspond to one standard deviation. All values represent **an area-weighted** average from 66°-82°N.